Microprismatic plane-focusing Fresnel lenses for light concentration in solar photovoltaic modules

E.E. Antonov[1], S.V. Kondratenko[2], V.S. Lysenko[3], V.V. Petrov[1], V.N. Zenin[1]

[1]*Institute for Information Recording, National Academy of Sciences of Ukraine*
2, Shpak str., 03113 Kyiv, Ukraine
[2]*Taras Shevchenko National University of Kyiv, 64/13, Volodymyrska str., 01601 Kyiv, Ukraine*
[3]*Institute for Semiconductors Physics, National Academy of Sciences of Ukraine*
41, prospect Nauky, 03680 Kyiv, Ukraine
Corresponding author e-mail: antv1947@gmail.com

Abstract. An algorithm has been developed for modeling the parameters of microprismatic specialized plane-focusing Fresnel lenses. Such lenses are more effective for application in photovoltaic modules for concentration of sunlight compare to the traditional point-focusing Fresnel lenses. The technical parameters of photovoltaic modules with these lenses were investigated. The method for manufacturing above lenses by diamond cutting technique and subsequent thermal pressing of silicone blanks is proposed. Some samples of specialized plane-focusing microprisms, which are made using our simulation results, have been experimentally investigated.

Keywords: microprismatic structure, modeling of plane-focusing optics, sunlight-to-electricity conversion.

https://doi.org/10.15407/spqeo26.02.188
PACS 07.60-j, 42.79-e, 85.60-q

Manuscript received 29.11.22; revised version received 12.01.23; accepted for publication 07.06.23; published online 26.06.23.

1. Introduction

Currently, applied research is being actively carried out to create photovoltaic modules for concentrated solar radiation [1]. The main idea here is to use the modern photoelements, in particular three-stage ones based on gallium arsenide or $A^{III}B^{V}$ compounds instead of traditional silicon amorphous photocells, but at a much smaller working surface, to improve efficiency of solar light photovoltaic transformation. It is claimed [2, 3] that more expensive, but much more efficient photovoltaic multi-junction cells can function effectively at a significant multiplicity of light concentration, even up to thousands of times. Such modules will be economically profitable, when the light multiplicity (or reduction of photovoltaic working area) is higher than the price increase for a single photovoltaic cell. Recent results of solar cell efficiencies listed in [4] showed that the GaAs solar cell has a measured record of 29.3 % efficiency under 49.9-suns, and the four-junction AlGaInP/AlGaAs/GaAs/GaInAs solar cell holds even the highest record of 47.1% under 143-sun irradiation.

There are numerous economic estimates (see, for example, [5]), according to which in the nearest future the photoelectric power industry with concentrated sunlight can become not only the most cost-effective among other photovoltaic (PV) devices, but also compete with the existing traditional sources in terms of the cost of generated electricity. Creation of concentrator modules enables to reduce the consumption of semiconductor materials to generate a given electrical power, because this consumption is proportional to the concentration multiplicity.

The concentration of light fluxes can be achieved by applying different mirrors, linear cylindrical focusing lenses, or by Fresnel lenses. However, a high concentration multiplicity of a range from hundreds to several thousands can be achieved only with Fresnel lenses. So, in this paper, we will focus just on the high-concentration photovoltaic (HCPV) modules with micro-prismatic Fresnel lenses.

Non-uniform irradiation distribution over the PV-surface is one of the most challenging issues for solar cells with concentration of light. Many researches, for example, [6–8], are devoted to studying this phenomenon. It is well-known that the longer the focal distance, the focal spot is larger, and the more uniformly the solar cell is illuminated. However, with an increase in the focal spot diameter, the solar cell area should be enlarged accordingly. On the other hand, when the focal distance is reduced, the illumination inhomogeneity at various points of photocell surface increases, which leads to an increase of the side currents inside the structure between the HCPV cascades, and accordingly, the ohmic losses increase [9]. When the illuminated regions excessively generate huge currents, they also are overheated. This process decreases the electrical output, because the central areas of solar cells do not operate properly, which is caused by the rising cross-ohmic currents. This, in turn, causes a dissipation of generated electrical power. At the same time, a shadow (low-intensity) effect that occurs at the peripherical parts of solar cells might cause limitation of the photocurrent in the connected cell parts and therefore cause limitation of cell performances.

Currently, the Fresnel optics applied in HCPV modules are mostly the traditional point-focusing lenses [10], which produce non-uniform irradiation distribution for concentrated sun-light. The typical known focusing scheme [9] is illustrated in Fig. 1a. Many researchers try to diminish this effect [6–10]. However, it is possible to completely solve the problem of internal ohmic losses caused by non-uniform irradiation in HCPV modules by applying for sun-light concentration the new transforming Fresnel lenses [11] that create a uniformly illuminated light circle in the lens focal plane (Fig. 1b).

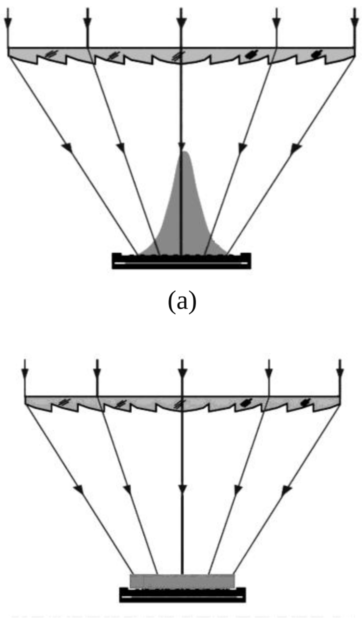
(a)

(b)

Fig. 1. Light beam transformation by Fresnel lenses: a) point-focusing lens [9], b) transforming plane-focusing Fresnel lens [11].

Another important feature of plane-focusing optics [11] is the ability to reduce significantly the focal distance f of concentrator lens. For example, the lens with optical diameter D_L = 56 mm, which corresponds to traditional rectangular lens of size ~40×40 mm [9], can be made with diminished focal distances f (from usual 75…105 mm to 20…25 mm). These f-values for transforming lenses [11] are restricted only by the limit angles $\alpha_{k\,\max}$ [12] of refractive microprism zones. Accordingly, the diminished f-value leads to reducing the dimensions of concentrator single cell and the total thickness of HCPV module, which is especially important for space solar photocells.

So, the main aim of our paper is to deliver an algorithm for creating plane-focusing Fresnel lenses for solar concentration modules, which is specially adapted for mass manufacturing of such lenses by thermo-pressing method. Other aim is to investigate the main properties of created lenses for possible photovoltaic modules.

2. Algorithm for modeling Fresnel transforming optics

Earlier in our paper [11], an algorithm was proposed for modeling the parameters of transforming microprismatic optics. In their focal plane, these Fresnel lenses form a light circle of required radius r_V with an almost homogeneous illumination distribution. The scheme of light refraction for these lenses is shown in Fig. 2, where f is the lens focal distance; n_0 and n_1 are the refractive indices of the medium and the material of microprism, accordingly; R_k is the radius of annular prismatic zones $k = 1, 2, 3, \ldots, N$ of the lens; ΔR_k is the width of the refractive k-zone of the lens in the direction of axis X^0; $r_V = R_1$ is the outer radius of the light spot in the focal plane; γ_k is the angle of observation for k-zone from the focus F; α_k is the prism refractive angle and h_k is the relief depth for the k-zone.

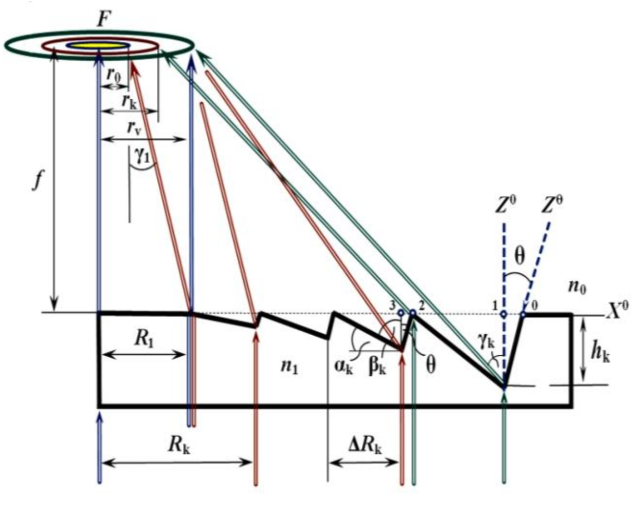

Fig. 2. Modified scheme of Fresnel plane-focusing structure with variable pitch ΔR_k and depth h_k of microrelief.

We realize our calculation results for lens manufacturing by a diamond cutting method [12, 13]. This technique ensures formation of operating facets with an exceptional geometrical accuracy and mirror-like surface quality. Recently, we have successfully applied this method for manufacturing the microprism structures for computer eye-glasses [14] and for creating the lenses for moving objects control systems [15].

The algorithm for calculating the focusing structure suitable for implementation of diamond-cutting method involves, firstly, the setting of central lens zone, which in the process of lens manufacturing remains flat. The size R_1 of this zone is determined primarily by technological requirements: during diamond-cutting the speed of rotation of the cutting tool at the point $R_1 = 0$ is zero; hence the value of R_1 cannot be zero or very small. A parallel light beam passes through this flat zone of radius R_1 without refraction, thus at the center of the focal plane a flat illuminated area with radius $r_V = R_1$ is formed. All other annular refractive lens zones with inclined flat surfaces of radii R_k and widths ΔR_k should focus the transmitted light onto this single central circle of radius r_V at the lens focal plane.

After setting the radius R_1 of this central zone the angle γ_1 of ray inclination by the first prismatic zone is determined at this point $R = R_1$. This value γ_1 determines the refraction angle α_1 of circular zone $k = 1$ according to Snell's law [16]:

$$\gamma_1 = \mathrm{arctg}(R_1/f), \qquad \alpha_1 = \mathrm{arctg}\{\sin\gamma_1/(n_1/n_0 - \cos\gamma_1)\}. \tag{1}$$

By this refraction angle α_1, the ray from the point $R = R_1$ is directed to the center of the image formed by the lens in the focus plane F. According to proposed calculation model, this angle α_1 determines the inclination angle γ_1 for all rays passing through the first annular microprism zone of width $\Delta R_1 = (R_2 - R_1)$. The central R_1 and first inclined zone R_2 are formed with the same width $\Delta R_1 = (R_2 - R_1) = R_1$ which ensures focusing the passed beams into a single light circle of radius $r_V \approx \Delta R_1 = R_1$ (see Fig. 2). After determining the radius R_2 at the point $R = R_2$ the angle γ_2 of ray inclination by the second prismatic zone $k = 2$ is determined; and then the relief parameters for the zones $k = 3, 4, \ldots, N$ are calculated.

Our algorithm [11] for obtaining a homogeneous spot at the first stage supposes formation a not-illuminated "dark" area of variable radius r_j in the center of focal spot. It is necessary for compensation of a light beam concentration in the narrow central area of the round focal spot. This feature is explained by transformation of larger annular light fluxes into the light rings with the smaller diameters under their focusing. This process of light beam concentration is considered in detail in our previous paper [17]. So, the refractive angles α_k are calculated with these "dark" zones in mind.

Then optimization of the focusing process (FO) is necessary [11] to achieve the homogenization effect. This process means that the corresponding prismatic k-zones of the lens with radii R_k and widths ΔR_k should direct the refracted light beams into certain focal annular areas with the widths $W_j = r_V - r_j$, where $j = 0, 1, 2 \ldots M$. The width of annular illuminated areas W_j will be considered as the nominal relief pitch of microrelief, which is necessary to further calculate the refractive parameters of prismatic zones. The number M of the groups of lens zones is defined by the light diameter D_L and the nominal pitch W_j. Usually, the value of $M = 3\ldots4$ is enough to obtain focal spot homogeneity.

The number of k-zones in the lens is defined by the focal ring width W_j and the lens diameter D_L. Under optimization process all k-zones of the lens are grouped into the prismatic groups, each j-group is related to certain pitch W_j. It is assumed that the central "dark" areas of radii r_j will be illuminated by diffracted transmitted light, as well as by diffuse scattering of the light reflected from the lens forming plate and chaotically refracted at the relief defects.

At the next modeling stage, the process of light beam narrowing should be taken into account by applying the appropriate correction of the pitch ΔR_k and the depth h_k of microrelief for a lens with a necessary light diameter $D_L = 2R_L$. We will call this process as zone correction (ZC). As the angles α_k increase, each k-zone forms a narrower ring in the focal plane with outer radius r_k instead of r_V and with the width $\Delta r_{jk} = r_k - r_j$. This process is obviously illustrated in Fig. 2. To expand the refracted annular light beam from the radius r_k to radius r_V, it is necessary to increase in proportion the radii of lens refractive zones $R_k = W_j + \Delta R'_k$ and, accordingly, the depths of microrelief $h_k = W_j \mathrm{tg}\,\alpha_k + \Delta h'_k$, where a nominal lens relief pitch $W_j = r_V - r_j$ is different for various j-groups of prismatic zones.

Indeed, the method proposed earlier in our work [11] accurately simulates the focusing structures only for large aperture numbers $f/D_L > 1.5\ldots2.0$, when the refraction angles of microprisms α_k are rather small. For larger angles α_k it is necessary to change the widths of zones ΔR_k and the depths of relief h_k to compensate the narrowing of light fluxes. For any angles α_k and γ_k, the necessary correction of the width $\Delta R'_k$ and the depth $\Delta h'_k$ of the microrelief (the so-called ZC) for each j-group can be defined as:

$$\Delta R'_k = W_j\, \mathrm{tg}^2\alpha_k\, \mathrm{tg}\gamma_k / (1 - \mathrm{tg}\alpha_k \mathrm{tg}\gamma_k),$$
$$\Delta h'_k = \Delta R'_k\, \mathrm{tg}\,\alpha_k. \tag{2}$$

The variable pitch R_k and depth h_k of the microrelief are:

$$R_k = W_j (1 + \mathrm{tg}\alpha_k \mathrm{tg}\gamma_k)/(1 - \mathrm{tg}\alpha_k \mathrm{tg}\gamma_k),$$
$$h_k = W_j\, \mathrm{tg}\alpha_k (1 + \mathrm{tg}\alpha_k \mathrm{tg}\gamma_k)/(1 - \mathrm{tg}\alpha_k \mathrm{tg}\gamma_k). \tag{3}$$

The next problem – uniformly illuminated light spot in the focal plane has a rather large radius $r_V > 5\ldots10$ mm; therefore the restraining factor exists: the used diamond cutters have a cutting edge that usually is no more than 1.2...1.5 mm. So, the length of inclined working surfaces of microprisms $\Delta R_k / \cos\alpha_k$ or the widths of each prismatic zone $\Delta R_k = (R_{k+1} - R_k)$ cannot be larger than ~ 1.2 mm. To eliminate this limitation, it is proposed [11] to form each of zones $k = 1, 2, 3, ..., N$ from several similar constituent microprismatic elements N_c with the same refractive angles α_k and widths ΔR_{kc}. The total width $\Sigma\,\Delta R_{kc}$ of prismatic elements for each of these composed k-zones in the sum should be equal to the width ΔR_k. The value of $\Delta R_k = \Sigma\,\Delta R_{kc}$ for each zone k is defined by an appropriate variation of the relief depth h_k and the number of constituent elements N_c.

At the final stage of simulation, with account of the stated light focusing optimization scheme (FO) and width zone correction (ZC) by using the formulas (2) and (3), the geometrical parameters of necessary transforming Fresnel lens can be calculated.

The offered algorithm allows modeling the lens that forms a uniformly illuminated area in the focal plane at any focal distance f. We will start calculating the parameters of the lens with the minimum possible focal distance f that is essential for solar modules. However, for a smaller f values the prism refractive angles α_k approach to their limiting value $\alpha_{k\,\max}$, at which the total internal reflection [16] occurs for transmitted light beams. Therefore, the light transmittance τ^R also decreases with decreasing f, but the thickness of concentrator module, made from these lenses, also decreases. This will allow one to minimize the size of concentrator module that is decisive when constructing photovoltaic devices.

To create the lens for solar concentrators, we will calculate the prismatic structure with the focal distance $f = 25$ mm and light diameter $D_L = 50$ mm, which enables to form the round uniformly illuminated area with the radius $r_V = 1.5$ mm in the focal plane. So, this lens # 25-c can ensure the sunlight concentration multiplicity $k_c \sim 280$. The simulation showed that for above lens #25-c the correction procedure realizes 18 prismatic zones corresponding to 3 values of $W_j = 1.0$, 0.7 and 0.4 mm, each of W_j contribute by 14, 2 and 2 prismatic k-zones, accordingly. The details of calculation can be seen in Appendix *A*, some obtained data have been shown also in Fig. 3a.

The proposed optimization scheme FO of light beams focusing for the lens #25-c is illustrated in Fig. 3b: created prismatic zones # 1–14 reflect light beams to the focal light ring of width $W_1 = r_V - r_0 = 1.0$ mm, zones #15–16 – to the ring of $W_2 = r_V - r_1 = 0.7$ mm, and zones #17–18 reflect light beams to the ring of width $W_3 = r_V - r_2 = 0.4$ mm ($M = 3$). We will call this scheme of focusing optimization as FO: 0.5 (14)–0.8 (2)–1.1 (2). Under above conditions the focal light distribution has "dark" central area of radius $r_0 = 0.5$ mm and three light peaks for radii $r_j = 0.5$, 0.8 and 1.1 mm with the outer radius $r_V = 1.5$ mm. Our previous experience testifies that in practice for above "three-peak" FO-scheme the lens manufactured using diamond cutting, due to diffuse scattering demonstrates the focal light distribution that is practically flat.

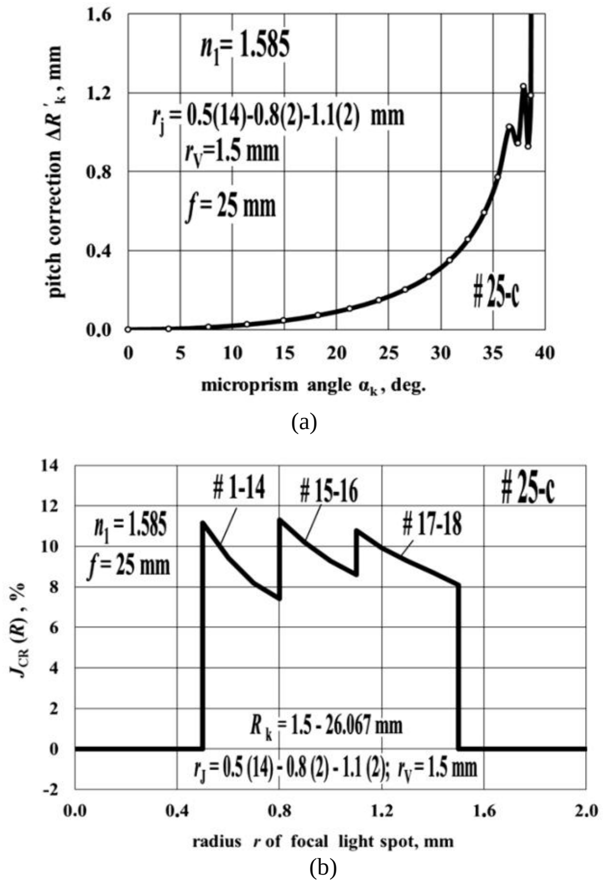

Fig. 3. Parameters of the lens # 25-c with the focal distance $f = 25$ mm that forms flat focal light circle: a) pitch correction, b) scheme of focusing optimization.

Using the obtained data on FO and ZC, modeling the lens relief depth h_k depending on radius R_k can be performed. The calculated structure of the relief for above lens-concentrator # 25-c for $R_k < 26.067$ mm is shown in Fig. 4a. The general view of real plane-focusing lens # 25-c, made using diamond micro-cutting, is illustrated in Fig. 4b.

The refractive indices $n_1(\lambda)$ for the formula (1) were used from the data [18]. Simulation of parameters was performed for polycarbonate ($n_1 = 1.585$) for the wavelength $\lambda = 0.532$ μm, which is most suitable for solar concentrators systems. The details of calculation are contained in Appendix *B*.

We have modulated lens prismatic zones having refractive angles $\alpha_k \approx 3.9…38.6$ deg. This lens-concentrator # 25-c with the focal distance $f = 25$ mm has a fairly high total light transmission $\tau^R = 77.56$ % defined by the Fresnel refraction [16] of light beams refraction at the both sides of relief forming plate. The calculated τ_k^R for each prismatic k-zone of the lens depending on the radii R_k have been shown in Fig. 5a.

In the case of microprisms with reverse angle $\theta > 0$ (Fig. 2), which is necessary to simplify the lens manufacturing process by using the thermo-pressing method [16],

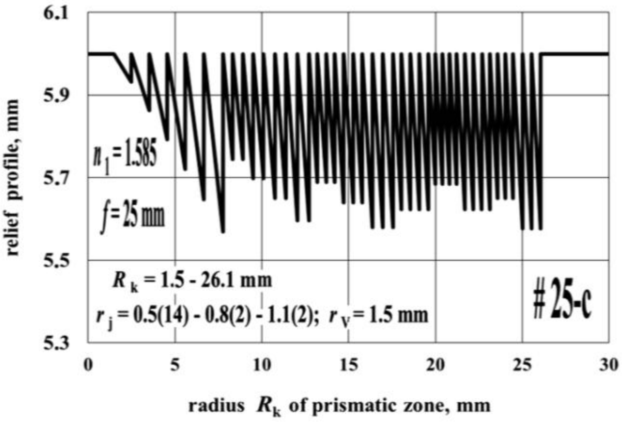

(a)

(b)

Fig. 4. Structure of microrelief inherent to the lens # 25-c with the focal distance f = 25 mm, which forms a focal light circle of the radius r_V = 1.5: a) modulated relief profile, b) real structure of the lens.

another reason exists for diminishing a light transmission – the light beam vignetting with appropriate coefficient τ_k^V. It is easily to calculate (see Fig. 2 that the value τ_k^V = (zone length $_{1\text{-}2}$) / (zone length $_{0\text{-}2}$), thus:

$$\tau_k^V = 1/\left(1 + \text{tg}\alpha_k \text{tg}\theta\right). \quad (4)$$

The total light beams transmission for each k-zone can be obtained as $\tau_k^S = \tau_k^R \cdot \tau_k^V$, where τ_k^R values are calculated by known Fresnel formulas [12] and values τ_k^V are calculated according to the formula (4). The obtained values τ_k^S *versus* radii R_k are shown also in Fig. 5a. Note that the lens-concentrator # 25-c due to above vignetting τ_k^V, depending on the prismatic angle α_k and on the reverse angle θ = 3 deg, has a total light transmission τ^S that is diminished to the value τ^S = 74.67%, as compared to the above refraction value τ^R = 77.56%.

For a similar lens-concentrator # 22, but with the larger focal distance f = 50 mm, the total light transmission τ^R = 89.20% even up to the light diameter $D_L \approx$ 50 mm due to the smaller refractive angles α_k and diminished refraction losses τ_k^R for every lens radius R_k. For this lens, the scheme providing focusing optimization is FO: 0.5(17)–0.8(3)–1.1(5). Fig. 5b illustrates the transmission values $\tau_k^S = \tau_k^R \cdot \tau_k^V$ and τ_k^R for the lens # 22. The diminished total transmission τ^S is equal to 87.02% due to the vignetting τ_k^V for this lens.

The obtained data indicate that diminishing the focal distance f markedly diminishes the light transmission $\tau_k^S = \tau_k^R \cdot \tau_k^V$ mainly due to the enlarged refraction losses τ_k^R. However, this process can also diminish the total thickness and the weight of single solar concentrator cell, constructed with these lenses, which is more important. This fact should be taken into account when constructing the solar concentrator modules.

Calculated according to the formulas (2) and (3) zone enlargement is rather large as compared to the nominal pitches W_j (Fig. 6a). The values of ΔR_k for large radii R_k are several centimeters, but operation cutting edge of diamond tool is ~ 1.5 mm.

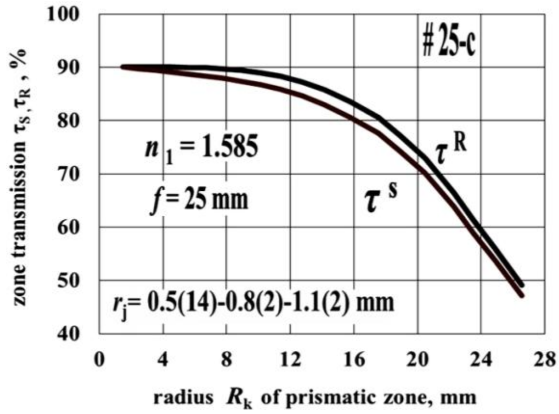

(a)

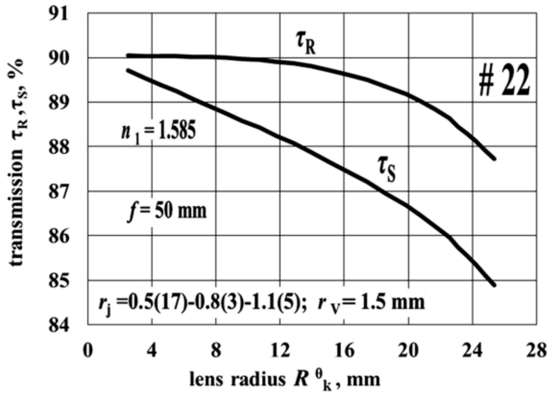

(b)

Fig. 5. Calculated light transmission τ_k^R, τ_k^V for each k-zone of the lens depending on the radius R_k: a) lens #25-c with f = 25 mm, b) lens #22 with f = 50 mm.

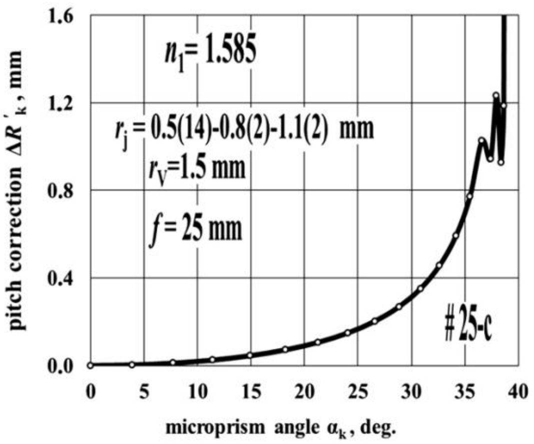

(a)

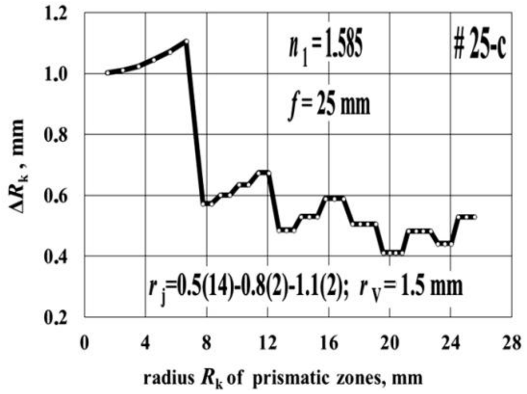

(b)

Fig. 6. Calculated pitch enlargement $\Delta R_k / W_j$ (a) and relief pitch ΔR_k for each k-zone of the lens depending on the radius R_k (b) for the lens #25 with f = 25 mm.

Therefore, taking in mind the future diamond cutting process for lens manufacturing, only zones #1–6 of the lens #25-c up to radius R_7 = 7.762 mm each can be formed using the single prismatic element (see Fig. 4a and Fig. 6b); zones #7–10 should be made from two identical microprisms; refractive zones #11–13 and zones #17–18 – from three similar prismatic elements, and zones #14–16 each should be made from four similar prismatic elements. In this case, all zone widths ΔR_k are less than ~1.1 mm, and the simulated lens profile can be formed using the diamond cutting method [14].

According to our traditional algorithm [11], the diamond cutter movement, when manufacturing, is performed along the axis X^0 (Fig. 2). This movement is responsible for formatting the lens prism operation surfaces of widths ΔR_k.

This axis X^0 is strictly perpendicular to the plane of rotation of relief forming plate or to the direction Z^0, responsible for forming the relief depths h_k.

During this process, the complementary angle $\beta_k^{\theta} = 90° - \alpha_k$ is very important, which sets the necessary angle of inclination ξ_k for the cartridge with diamond cutter of angle α_G to the axis X^0: angle $\xi_k = \beta_k^{\theta} - \alpha_G$.

3. Manufacture and testing the lenses for solar concentration modules

A well-established optical production technology used for generation of any lenses is ultra-precision machining (UPM) [19]. The UPM method using a diamond tool enables to fabricate lenses with exceptional geometrical accuracy and mirror-like surfaces. Such lenses meet the highest needs of optical industry. The physical set-up of UPM machine [19] is shown in Fig. 7a. The used technology of direct diamond cutting by computer control being able to guide the tool along the feature as desired. During this process, the rake face of the tool is kept orthogonal to the cutting direction at every point [20]. For this demonstration the PMMA substrate of size 75×25 mm was used. This plate was attached to the fixture using wax. After the substrate was mounted, it was trimmed to ensure the plane of machining to be flat, using a diamond tool of radius R_G = 1 mm. For the relief shaping tool, a natural monocrystalline diamond tool was used, with a 12 μm nose radius, 20 deg included angle, 120 deg opening angle and 15 deg front clearance angle. To avoid undesired interactions between the other faces of the tool with the facets that are not being machined, the tool is set with the negative 14-deg rake angle [20]. It gives more space to the front clearance of the tool, avoids deforming the facets at the corners, also allows maneuver the tool without clashing into the succeeding facets of the lens.

We will call this technology as diamond micro-cutting (DMC) and also will use it to fabricate our simulated microprisms. This technique was effectively developed [11] in the Institute for Information Recording of National Academy of Sciences of Ukraine (IIR). The general view of our installation is shown in Fig. 7b. A diamond cutter tool is hold in special cartridge, which allows moving the diamond cutter of cutting angle α_G along axis X and Z with calculated inclination (clearance) angle β. Computer control allows setting the necessary cutter positions in this coordinate system by few micrometers accuracy (no more than ~5 μm). The diamond cutter for shaping relief of simulated lens #25-c has almost similar to [20] parameters: 8 μm nose radius, 46 deg front angle α_G, clearance angle β can be changed from 5 up to 40 deg according to simulation scheme # 25-c (Appendix *B*) and 86 deg opening angle.

The first samples of lenses of 1970-th for solar concentration modules were not perfect. Harmon [21] presented experimental and analytical methods to determine the efficiency and intensity variations for circular Fresnel lens as a solar concentrator. It was found experimentally that these "old" lenses were an inefficient concentrator with losses that begin at 20% and rose to about 80% as the focal distance decreased. However, the modern lenses [2, 9] of 2000-th showed solar light efficiency as high as ~89% for the focal distance f = 75 mm and lens sizes 40×40 mm.

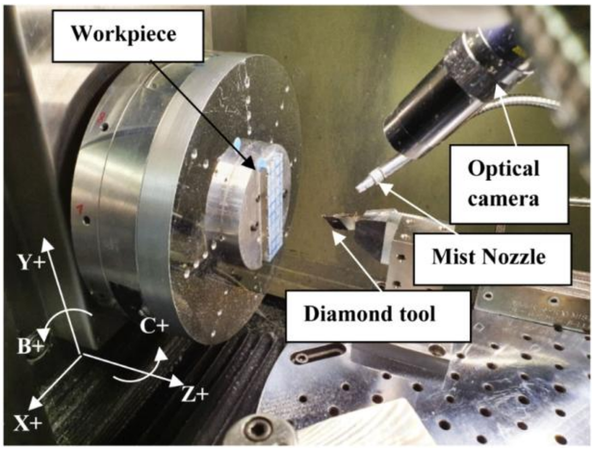

(a)

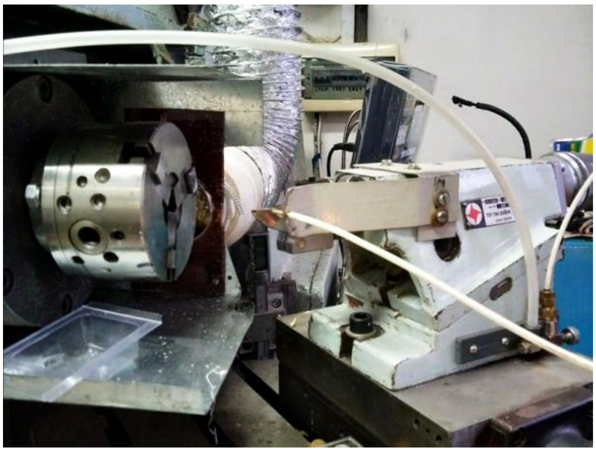

(b)

Fig. 7. Physical set-up [20] for ultra-precision machining with diamond tool (a), experimental diamond micro-cutting installation [16] of the Institute for Information Recording of National Academy of Sciences of Ukraine (b).

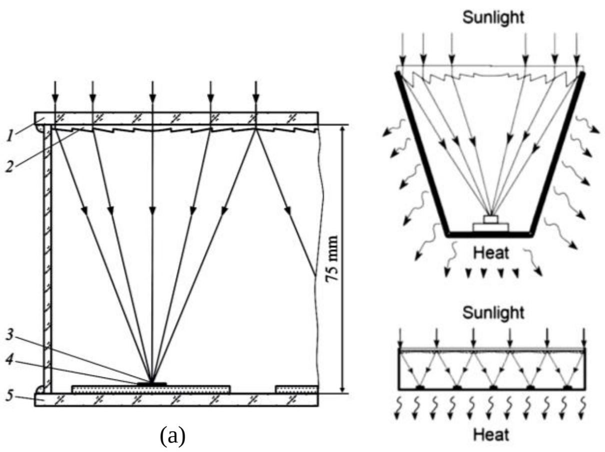

(b)

Fig. 8. Scheme of concentrator module. (a) Cross section of concentrator module [9]: *1* – lens panel base made of glass, *2* – Fresnel microprisms made of silicone, *3* – focused sun beams, *4* – solar cell mounted on a metal base, *5* – glass base of solar cell panel; (b) large- and small-aperture solar modules [2].

The typical scheme of a single photo-converter module [9] with a Fresnel lens for high light beam concentration is shown in Fig. 8a. Protection from the environment is provided by the front and rear glass panels, as well as by the module walls.

In this design, the circular microprismatic Fresnel lenses with constant relief pitch $S = 0.25$ mm are used. This pitch profile was chosen as caused by limitations imposed by technology of manufacturing the precise metal matrices for Fresnel lenses [9]. The angle of inclination of each microprism is calculated with account of the condition that a beam incident along the normal to the base of the lens is refracted in the middle of the oblique surface and crosses the optical axis at the module focal plane at the stated focal distances $f = 95$, 80, 65 and 55 mm. The lenses [9] were made from two-component silicone “ELASTOSIL RT 604”. This plastic demonstrated a good ability to function in solar concentrator modules for a long time under various environmental conditions. The photocell surface illumination is non-uniform, which is caused by the known properties inherent to traditional Fresnel lenses of spherical type.

Providing an acceptable thermal regime of solar cells for solar photovoltaic modules is one of the problems during their design optimization [2]. The heat dissipation for HCPV module was evaluated [9] by initial dilution heat flow through the copper plate and subsequent discharge into the environment due to radiation and contact with the surrounding air. For smaller in-size concentrators (Fig. 8b), an effective heat distribution is realized with thinner heat-sinking materials. The focal distance of such concentrators is shorter. Therefore, the consumption of structural materials for heat-spreading elements and module walls is much lower.

However, the negative influence of non-uniform illumination of HCPV module cannot be compensated by the usage of a more dense contact grid, because lateral currents arise between sub-cells inside this module [2]. Comparison of the large- and small-aperture area in these modules was carried out in [9]. It was found that smaller-in-area cells are preferable due to having lower ohmic losses, which diminishes the absolute currents flowing along shorter lateral paths.

A significant increase in the multiplicity of concentrated solar radiation in the cell center can lead to restrictions due to ohmic losses in the contact grid and due to local overheating the solar cell. Composite silicone-on-glass Fresnel lenses are characterized by excellent environmental stability, but for them, there exists such an insufficiently explored feature [2] as the influence of thermal regimes on optical efficiency at solar energy concentration. So, a reduction of internal ohmic losses is a key problem in the development of concentrator photovoltaic cells.

Therefore, the maximum possible optical efficiency of each individual module is achieved when using relatively “long-focus” lenses with small diameters of photocell ~1.7 mm. For the practical design of solar concentrator modules, the authors [9] applied two sizes of Fresnel lenses: 40×40 mm with the focal distance $f = 70$ mm and 60×60 mm with $f = 105$ mm. The diameter of photosensitive surface of photocell in the first case is 1.7 mm, in the second – 2.3 mm. When using Fresnel lenses of 40×40 mm, high efficiency of solar energy conversion is achieved with the photocells of ~2-mm diameter, which corresponds to a concentration multiplicity close to 500.

At the same time, usage of new plane-focusing lenses [11] can resolve easily the problem of diminishing lateral currents and ohmic losses. Our simulated lens #25-c has a fairly small focal distance $f = 25$ mm and provides uniform focal light spot distribution, decreasing totally the ohmic losses. In Fig. 9a, the image of a transformed light beam in the lens focus is shown. These data were obtained in the experimental study of this lens by using a collimated laser beam of the wavelength $\lambda = 0.532$ μm and beam diameter $D_S = 60$ mm. The optical scheme of this experimental setup was discussed in detail [17]. The profile of light spot in the focal plane for lens # 25-c of light diameter $D_L = 25$ mm and focal distance $f = 25$ mm is shown in Fig. 9b. This distribution was obtained similar to [17] by using the known programme "Jmage-J-1.53".

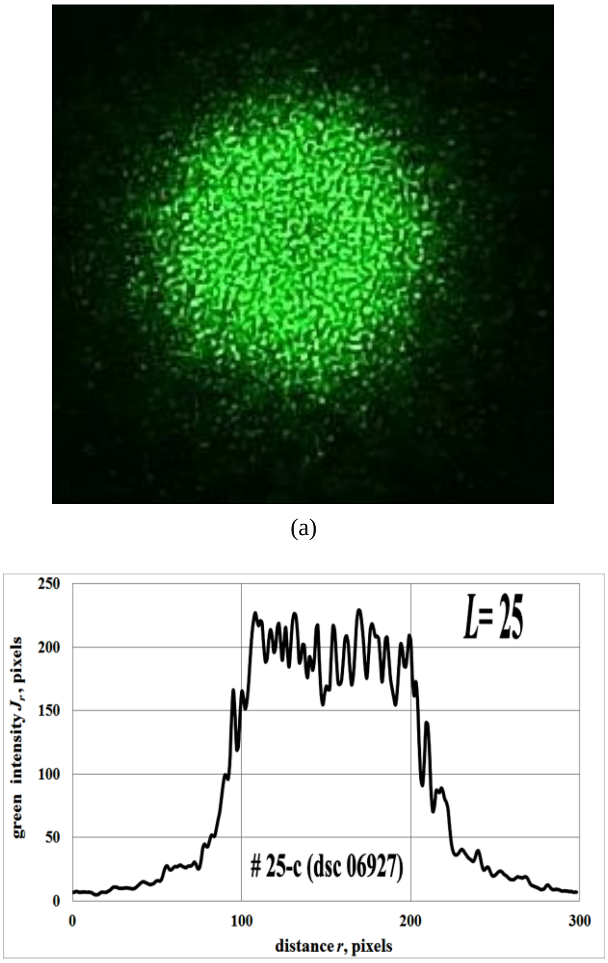

(a)

(b)

Fig. 9. Light spot in the focal plane for the lens # 25-c of light diameter $D_L = 25$ mm and focal distance $f = 25$ mm: measured light spot distribution (a), profile of focal light spot (b).

The light total transmittance τ^S decreases for such lenses with a small focal distance f due to enlarging the microprism refractive angles α_k that approach the limit values $\alpha_{k\,\max}$. Therefore, the optimal aperture numbers for plane-focusing lenses are $f/D_L \approx 1.5\ldots2.0$.

The created lenses can be effectively used in solar concentration modules. Computational and experimental data confirmed that the best variant for focusing the solar radiation beams on the sensitive surface of photodetector matrix is usage of transforming lenses-concentrators that create a uniformly illuminated light circle in the focal plane. These lenses are more effective in constructing a solar concentration module with minimal thermal and ohmic losses.

4. Conclusions

Computational and experimental data confirmed that usage of a new lens-concentrator that forms a uniformly illuminated light circle in the focal plane is the best variant of focusing solar radiation on the sensitive surface of photodetector matrix for creating the solar concentrator modules with minimal thermal and ohmic losses.

The algorithm of mathematical modeling of plane-focusing microprismatic lenses was developed to create the optimal Fresnel lenses for solar photovoltaic modules. The set of calculations was carried out for creating specialized plane-focusing lens-concentrators. The optical and geometric parameters for such specialized microprism lens-concentrators are specially adapted for mass manufacturing these lenses by using the thermo-pressing method.

According to the results of our simulation, the samples of specialized lens concentrators were manufactured from the optical polycarbonate by the diamond micro-cutting technique. The experimental study of optical and lighting characteristics of these samples showed the complete compliance of experimental data with theoretically obtained characteristics.

The total light transmittance for these lenses τ^S is decreasing, when diminishing the focal distance f due to enlarging the microprism refractive angles α_k and approaching them to the limit value $\alpha_{k\,\max}$. Therefore, the optimal aperture numbers for created plane-focusing Fresnel lenses are $f/D_L \approx 1.5\ldots2.0$. The proposed specialized lens-concentrators that transform the refracted light beams into a uniform light circle in the focal plane can be used effectively in optical concentrator modules for diminishing the ohmic currents and thermal losses; also they can be useful for minimizing the thickness of solar photocells.

Appendix A

Zone correction for transforming Fresnel lens: $r_V = 1.5$ mm; $r_j = 0.5$ mm (14 zones) - 0.8 mm (2) - 1.1 mm (2)

f = 25 mm, λ=0.532 μm ($n_1 = 1.585$), δ= 6.0 mm, $\alpha_{KK} = 39.118°$, $\tau_{Fr1} = 0.949$, $\tau_{Fr2} = 0.901$

$\Delta R'_k = \{W_j\, tg\alpha_k\, tg\gamma_k / (1 - tg\alpha_k\, tg\gamma_k)\}$; $\Delta h'_k = \{W_j\, tg^2\alpha_k\, tg\gamma_k / (1 - tg\alpha_k\, tg\gamma_k)\}$; $W_j = r_V - r_j$

 # 25-c

Zone		r_j	$R_k=R_{k-1}+\Delta R_k$	$\gamma_k=tg^{-1}(R_k/f)$		$\sin\gamma_i$	$\cos\gamma_i$	$\alpha_i=tg^{-1}\{\sin\gamma/(1{,}585-\cos\gamma_i)\}$		α + γ	$tg\,\alpha_k$	$tg\,\gamma_k$	$tg\alpha_k\,tg\gamma_k$	$\Delta R'_k=(h'_k tg_\alpha tg_\gamma/(1-tg_\alpha tg_\gamma))/tg_\alpha$	$\Delta R_k= W_j+\Delta R'_k$	$\Delta R'_k/W_j$	h'_k	h	$\Delta h'_k$	$\Delta h'_k/h'k$	$h_k=h'_k+\Delta h'_k$
#	$R_k - R_{k-1}$	[mm]	R_1=1.5 mm	rad	deg			rad	deg.					$h'_k = W_j\,tg\alpha_k$	mm		mm	mm x20	mm		
			1.500	0.000	0.00	0.0000	1.0000	0.000000	**0.000**	0.000				**0**	0.000	**1.000**	**0.000**	0	0.000	**0.000**	0.000
#1	**2.503 - 1.500**	0.5	1.500	0.040	2.29	0.0400	0.9992	0.068123	**3.903**	6.194	0.0682	0.0400	0.003	**0.0027**	1.003	**1.003**	**0.068**	1.365	0.000	**0.003**	0.068
#2	**3.514 - 2.503**	0.5	2.503	0.080	4.58	0.0799	0.9968	0.134936	**7.731**	12.311	0.1358	0.0801	0.011	**0.0110**	1.011	**1.011**	**0.136**	2.715	0.001	**0.011**	0.137
#3	**4.539 - 3.514**	0.5	3.514	0.120	6.87	0.1197	0.9928	0.199417	**11.426**	18.300	0.2021	0.1205	0.024	**0.0250**	1.025	**1.025**	**0.202**	4.042	0.005	**0.025**	0.207
#4	**5.584 - 4.539**	0.5	4.539	0.160	9.18	0.1595	0.9872	0.260708	**14.937**	24.114	0.2668	0.1615	0.043	**0.0450**	1.045	**1.045**	**0.267**	5.336	0.012	**0.045**	0.279
#5	**6.656 - 5.584**	0.5	5.584	0.201	11.49	0.1993	0.9799	0.318156	**18.229**	29.723	0.3293	0.2033	0.067	**0.0718**	1.072	**1.072**	**0.329**	6.587	0.024	**0.072**	0.353
#6	**7.762 - 6.556**	0.5	6.656	0.241	13.83	0.2391	0.9710	0.371319	**21.275**	35.107	0.3894	0.2462	0.096	**0.1060**	1.106	**1.106**	**0.389**	7.788	0.041	**0.106**	0.431
#7	**8.911 - 7.762**	0.5	7.762	0.283	16.20	0.2789	0.9603	0.419953	**24.062**	40.258	0.4465	0.2905	0.130	**0.1490**	1.149	**1.149**	**0.447**	8.930	0.067	**0.149**	0.513
#8	**10.113 - 8.911**	0.5	8.911	0.325	18.59	0.3189	0.9478	0.463978	**26.584**	45.178	0.5004	0.3364	0.168	**0.2024**	1.202	**1.202**	**0.500**	10.008	0.101	**0.202**	0.602
#9	**11.382 - 10.113**	0.5	10.113	0.367	21.03	0.3589	0.9334	0.503442	**28.845**	49.878	0.5508	0.3845	0.212	**0.2687**	1.269	**1.269**	**0.551**	11.016	0.148	**0.269**	0.699
#10	**12.733 - 11.382**	0.5	11.382	0.411	23.52	0.3991	0.9169	0.538486	**30.853**	54.375	0.5974	0.4353	0.260	**0.3514**	1.351	**1.351**	**0.597**	11.947	0.210	**0.351**	0.807
#11	**14.189 - 12.733**	0.5	12.733	0.455	26.07	0.4395	0.8982	0.569306	**32.619**	58.692	0.6400	0.4893	0.313	**0.4559**	1.456	**1.456**	**0.640**	12.800	0.292	**0.456**	0.932
#12	**15.780 - 14.189**	0.5	14.189	0.501	28.70	0.4803	0.8771	0.596129	**34.156**	62.859	0.6785	0.5476	0.372	**0.5911**	1.591	**1.591**	**0.678**	13.569	0.401	**0.591**	1.080
#13	**17.552 - 15.780**	0.5	15.780	0.549	31.43	0.5215	0.8532	0.619187	**35.477**	66.910	0.7127	0.6112	0.436	**0.7718**	1.772	**1.772**	**0.713**	14.254	0.550	**0.772**	1.263
#14	**19.578 - 17.552**	0.5	17.552	0.599	34.30	0.5635	0.8261	0.638701	**36.595**	70.892	0.7425	0.6821	0.506	**1.0262**	2.026	**2.026**	**0.743**	14.851	0.762	**1.026**	1.504
#15	**21.223 - 19.578**	0.8	19.578	0.644	36.91	0.6006	0.7996	0.652807	**37.403**	74.314	0.7646	0.7511	0.574	**0.9445**	1.645	**2.349**	**0.535**	10.705	0.722	**1.349**	1.257
#16	**23.154 - 21.223**	0.8	21.223	0.685	39.25	0.6326	0.7744	0.662740	**37.972**	77.218	0.7805	0.8169	0.638	**1.2316**	1.932	**2.759**	**0.546**	10.927	0.961	**1.759**	1.508
#17	**24.482 - 23.154**	1.1	23.154	0.723	41.42	0.6615	0.7499	0.669954	**38.386**	79.803	0.7922	0.8822	0.699	**0.9282**	1.328	**3.320**	**0.317**	6.337	0.735	**2.320**	1.052
#18	**26.067 - 24.482**	1.1	24.482	0.752	43.09	0.6831	0.7303	0.674281	**38.633**	81.718	0.7992	0.9353	0.748	**1.1843**	1.584	**3.961**	**0.320**	6.394	0.947	**2.961**	1.266
			26.067	0.806	46.20	0.7217	0.6922	0.679821	**38.951**	85.147	0.8084	1.0427	0.843	**8.0453**	9.545	**6.364**	**1.213**	24.251	6.504	**5.364**	7.716

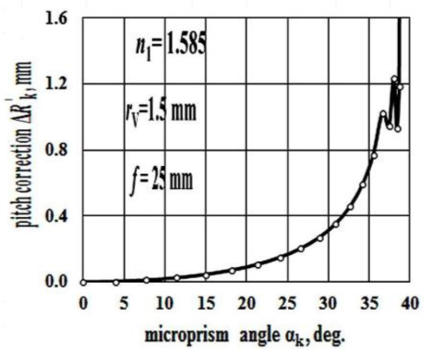

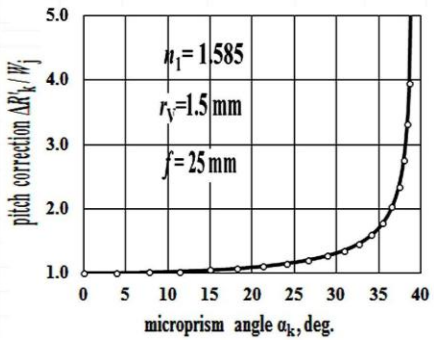

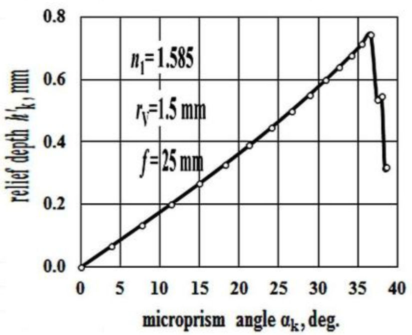

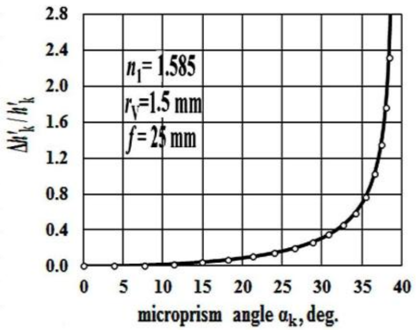

Appendix B (part 1)

$f = 25$ mm, $\lambda = 0.532$ μm ($n_1 = 1.585$), $r_V = 1.5$ mm, $\delta = 6.0$ mm, $\alpha_{k\,max} = 39.118$ deg., $\tau^R(Fr1) = 0.949$; $\tau^R(Fr2) = 0.901$. $\tau^V_k = 1/(1 + tg\alpha_k\, tg\theta)$

$\Delta R'_k = W_j\, tg\alpha_k\, tg\gamma_k / (1 - tg\alpha_k\, tg\gamma_k)$ $\Delta R^{\theta}_k = \Delta R_k \cos\theta + (h_k - h_{k-1}) \sin\theta$ $h_k = W_j\, tg\alpha_k \{1 + tg\alpha_k\, tg\gamma_k / (1 - tg\alpha\, tg\gamma)\}$

n	n		range	$\Delta R_k / W_j$	$R_k = R_1 + \Delta R_k$	$\gamma_k = tg^{-1}(R_k/f)$		$\sin\gamma_k$	$\cos\gamma_k$	$\alpha_k = tg^{-1}\{\sin\gamma/(1{,}584 - \cos\gamma_k)\}$		$\Delta R_k = h / tg\alpha_k$	$\Delta L_k = \Delta R_k / \cos\alpha_k$	$\beta = 90 - \alpha$	h	$\gamma + \alpha$	$\tau^R(Fr2)$
ΔR_k	Zone	r_j	mm		R_1=1,5mm	rad.	deg.			rad.	deg.	mm	mm		μm	deg.	a.u.
			1,500 - 0,000		0,000	0,000	0,00	0,0000	1,0000	0,000000	0,000						
	1	0,5	2,503 - 1,500	1,000	1,500	0,040	2,29	0,0400	0,9992	0,068123	0,000	1,00252	1,00	90,000	0,0	2,29	0,901
1	2	0,5	3,514 - 2,503	1,003	2,503	0,080	4,58	0,0798	0,9968	0,134922	3,903	1,01145	1,02	86,097	68,4	8,48	0,900
2	3	0,5	4,539 - 3,514	1,011	3,514	0,120	6,87	0,1197	0,9928	0,199431	7,730	1,02416	1,04	82,270	137,3	14,60	0,900
3	4	0,5	5,584 - 4,539	1,025	4,538	0,160	9,18	0,1595	0,9872	0,260674	11,427	1,04595	1,08	78,573	207	20,60	0,900
4	5	0,5	6,656 - 5,584	1,045	5,584	0,201	11,50	0,1993	0,9799	0,318173	14,936	1,07177	1,13	75,064	279	26,43	0,900
5	6	0,5	7,762 - 6,656	1,072	6,656	0,241	13,83	0,2391	0,9710	0,371334	18,230	1,10684	1,19	71,770	353	32,06	0,899
6	7	0,5	8,911 - 7,762	1,106	7,763	0,283	16,20	0,2790	0,9603	0,419999	21,276	0,57326	0,63	68,724	431	37,47	0,897
7		0,5			8,336	0,283	16,20	0,2790	0,9603	0,419999	24,064	0,57326	0,63	65,936	256	40,26	0,897
8	8	0,5	10,113 - 8,911	1,149	8,909	0,324	18,59	0,3188	0,9478	0,463928	24,064	0,60158	0,67	65,936	256	42,66	0,894
9		0,5			9,511	0,324	18,59	0,3188	0,9478	0,463928	26,581	0,60158	0,67	63,419	301	45,17	0,890
10	9	0,5	11,382-10,113	1,202	10,112	0,367	21,03	0,3589	0,9334	0,503422	26,581	0,63549	0,73	63,419	301	47,61	0,890
11		0,5			10,748	0,367	21,03	0,3589	0,9334	0,503422	28,844	0,63549	0,73	61,156	350	49,88	0,883
12	10	0,5	12,733-11,382	1,269	11,383	0,411	23,53	0,3992	0,9169	0,538526	28,844	0,67456	0,79	61,156	350	52,37	0,883
13		0,5			12,058	0,411	23,53	0,3992	0,9169	0,538526	30,855	0,67456	0,79	59,145	403	54,38	0,872
14	11	0,5	14,189-12,733	1,351	12,732	0,455	26,07	0,4395	0,8982	0,569292	30,855	0,48596	0,58	59,145	403	56,93	0,872
15		0,5			13,218	0,455	26,07	0,4395	0,8982	0,569292	32,618	0,48596	0,58	57,382	311	58,69	0,872
16		0,5			13,704	0,455	26,07	0,4395	0,8982	0,569292	32,618	0,48596	0,58	57,382	311	58,69	0,857
17	12	0,5	15,780-14,189	1,456	14,190	0,501	28,71	0,4803	0,8771	0,596150	32,618	0,53058	0,64	57,382	311	61,32	0,857
18		0,5			14,721	0,501	28,71	0,4803	0,8771	0,596150	34,157	0,53058	0,64	55,843	360	62,86	0,857
19		0,5			15,251	0,501	28,71	0,4803	0,8771	0,596150	34,157	0,53058	0,64	55,843	360	62,86	0,835
20	13	0,5	17,552-15,780	1,591	15,782	0,549	31,44	0,5216	0,8532	0,619212	34,157	0,58929	0,72	55,843	360	65,59	0,835
21		0,5			16,371	0,549	31,44	0,5216	0,8532	0,619212	35,478	0,58929	0,72	54,522	420	66,91	0,835
22		0,5			16,961	0,549	31,44	0,5216	0,8532	0,619212	35,478	0,58929	0,72	54,522	420	66,91	0,805
23	14	0,5	19,578-17,552	1,772	17,550	0,599	34,29	0,5634	0,8262	0,638682	35,478	0,50640	0,63	54,522	420	69,77	0,805
24		0,5			18,056	0,599	34,29	0,5634	0,8262	0,638682	36,594	0,50640	0,63	53,406	376	70,89	0,805
25		0,5			18,563	0,599	34,29	0,5634	0,8262	0,638682	36,594	0,50640	0,63	53,406	376	70,89	0,805
26		0,5			19,069	0,599	34,29	0,5634	0,8262	0,638682	36,594	0,50640	0,63	53,406	376	70,89	0,771
27	15	0,8	21,223-19,578	2,026	19,576	0,644	36,91	0,6005	0,7996	0,652789	36,594	0,41197	0,52	53,406	376	73,50	0,771
28		0,8			19,988	0,644	36,91	0,6005	0,7996	0,652789	37,402	0,41197	0,52	52,598	315	74,31	0,771
29		0,8			20,399	0,644	36,91	0,6005	0,7996	0,652789	37,402	0,41197	0,52	52,598	315	74,31	0,771
30		0,8			20,811	0,644	36,91	0,6005	0,7996	0,652789	37,402	0,41197	0,52	52,598	315	74,31	0,729
31	16	0,8	23,154 21,223	2,349	21,223	0,685	39,25	0,6327	0,7744	0,662745	37,402	0,48302	0,61	52,598	315	76,65	0,729
32		0,8			21,706	0,685	39,25	0,6327	0,7744	0,662745	37,972	0,48302	0,61	52,028	377	77,22	0,729
33		0,8			22,189	0,685	39,25	0,6327	0,7744	0,662745	37,972	0,48302	0,61	52,028	377	77,22	0,729
34		0,8			22,672	0,685	39,25	0,6327	0,7744	0,662745	37,972	0,48302	0,61	52,028	377	77,22	0,729
35	17	1,1	24,482-23,154	2,759	23,155	0,723	41,42	0,6616	0,7499	0,669959	37,972	0,44181	0,56	52,028	377	79,39	0,664
36		1,1			23,597	0,723	41,42	0,6616	0,7499	0,669959	38,386	0,44181	0,56	51,614	350	79,81	0,664
37		1,1			24,039	0,723	41,42	0,6616	0,7499	0,669959	38,386	0,44181	0,56	51,614	350	79,81	0,664
38	18	1,1	26,067-24,482	3,320	24,481	0,752	43,08	0,6831	0,7304	0,674277	38,386	0,52925	0,68	51,614	350	81,47	0,614
39		1,1			25,010	0,752	43,08	0,6831	0,7304	0,674277	38,633	0,52925	0,68	51,367	423	81,72	0,614
40		1,1			25,539	0,752	43,08	0,6831	0,7304	0,674277	38,633	0,52925	0,68	51,367	423	81,72	0,614
					26,069	0,806	46,20	0,7217	0,6922	0,679823	38,633	0,52328	0,67	51,367	424	84,83	0,614

Appendix B (part 2)

 # 25-c

$X^{\theta}_{k} = \Sigma\, \Delta R^{\theta}_{k+1}$ $\Delta Z^{\theta}_{k} = h^{\theta}_{k} + \Delta R^{\theta}_{k+1}\, \mathrm{tg}\theta$ $Z^{\theta}_{k} = h^{\theta}_{k} + \Sigma\, \Delta R^{\theta}_{k+1}\, \mathrm{tg}\theta$

$\pi(R_2^2-R_1^2)$	$\pi(R_2^2-R_1^2)\,\tau^R$	S_N/S_Σ	τ^V_k	τ^S_k	$\pi(R_2^2-R_1^2)\,\tau^S_k$	$\beta^\theta_k=90-\alpha+\theta$	h^θ_k	ΔR^θ_k	X^θ_k	ΔZ^θ_k	Z^θ_k	τ^R(Fr2)	τ^S_k
mm²	mm²	%	a.u.	a.u.	mm²	deg	µm	mm	mm	mm	mm	a.u.	%
											x10		
7,0686	6,3660	0,53	1,0000	0,901	11,3101	93,00	0,00	1,0011	23,163	0,053	12,607	90,060	90,060
12,6059	11,3505	0,80	0,9964	0,897	17,0904	89,10	68,49	1,0101	22,153	0,122	12,763	90,041	89,720
19,1177	17,2120	1,08	0,9929	0,894	23,0755	85,27	137,49	1,0228	21,130	0,192	12,917	90,032	89,396
25,9074	23,3200	1,38	0,9895	0,891	29,5170	81,57	207,28	1,0445	20,085	0,263	13,068	90,013	89,069
33,2609	29,9296	1,71	0,9862	0,887	36,4131	78,06	279,38	1,0703	19,015	0,337	13,228	89,984	88,744
41,2124	37,0416	2,06	0,9830	0,884	44,0820	74,77	353,48	1,1053	17,910	0,383	13,389	89,880	88,355
50,1364	44,9816	1,19	0,9800	0,879	25,4169	71,72	431,59	0,5725	17,337	0,462	13,870	89,718	87,924
28,9926	26,0117	1,27	0,9771	0,877	27,1406	68,94	256,35	0,5725	16,765	0,288	11,818	89,718	87,667
31,0574	27,7758	1,41	0,9771	0,874	30,1837	68,94	256,35	0,6008	16,164	0,288	11,503	89,434	87,389
34,8121	30,9752	1,51	0,9744	0,867	32,1553	66,42	301,41	0,6008	15,563	0,335	11,639	88,978	86,705
37,0860	32,9985	1,67	0,9744	0,867	35,7363	66,42	301,41	0,6346	14,929	0,335	11,306	88,978	86,705
41,6465	36,7678	1,78	0,9719	0,858	37,9137	64,16	350,48	0,6346	14,294	0,386	11,464	88,285	85,809
44,1840	39,0080	1,97	0,9719	0,858	42,0181	64,16	350,48	0,6736	13,620	0,386	11,111	88,285	85,809
49,6763	43,3337	2,08	0,9696	0,846	44,4364	62,14	403,55	0,6736	12,947	0,429	11,289	87,232	84,584
52,5353	45,8277	1,57	0,9696	0,846	33,4388	62,14	403,55	0,4853	12,461	0,429	11,035	87,232	84,584
39,6188	34,5603	1,60	0,9675	0,844	34,0911	60,38	311,43	0,4853	11,976	0,337	9,859	87,232	84,401
41,1027	35,2345	1,65	0,9675	0,829	35,3218	60,38	311,43	0,4853	11,491	0,339	9,605	85,723	82,941
42,5865	36,5065	1,87	0,9675	0,829	39,8927	60,38	311,43	0,5299	10,961	0,339	9,327	85,723	82,941
48,1914	41,3112	1,89	0,9657	0,828	40,2856	58,84	360,49	0,5299	10,431	0,388	9,540	85,723	82,780
49,9602	41,7181	1,95	0,9657	0,806	41,7119	58,84	360,49	0,5299	9,901	0,391	9,262	83,503	80,635
51,7291	43,1951	2,24	0,9657	0,806	47,9160	58,84	360,49	0,5885	9,313	0,391	8,954	83,503	80,635
59,5261	49,7058	2,24	0,9640	0,805	47,8998	57,52	420,58	0,5885	8,724	0,451	9,246	83,503	80,496
61,7080	49,6890	2,32	0,9640	0,776	49,5935	57,52	420,58	0,5885	8,136	0,447	8,938	80,523	77,623
63,8900	51,4459	2,06	0,9640	0,776	43,9044	57,52	420,58	0,5057	7,630	0,447	8,673	80,523	77,623
56,6460	45,6129	2,11	0,9625	0,775	45,1533	56,41	376,52	0,5057	7,124	0,403	7,967	80,523	77,507
58,2573	46,9103	2,08	0,9625	0,775	44,4224	56,41	376,52	0,5057	6,619	0,403	7,702	80,523	77,507
59,8685	46,1510	2,14	0,9625	0,742	45,6180	56,41	376,52	0,5057	6,113	0,398	7,437	77,087	74,200
61,4798	47,3931	1,78	0,9625	0,742	37,9513	56,41	376,52	0,4114	5,702	0,398	7,006	77,087	74,200
51,2044	39,4721	1,81	0,9615	0,741	38,7417	55,60	315,43	0,4114	5,290	0,337	6,180	77,087	74,117
52,2708	40,2941	1,75	0,9615	0,741	37,4005	55,60	315,43	0,4114	5,290	0,337	6,180	77,087	74,117
53,3372	38,8992	1,79	0,9615	0,701	38,1482	55,60	315,43	0,4114	4,879	0,341	5,964	72,931	70,121
54,4036	39,6769	2,14	0,9615	0,701	45,6426	55,60	315,43	0,4824	4,396	0,341	5,458	72,931	70,121
65,1435	47,5096	2,19	0,9607	0,701	46,6697	55,03	377,52	0,4824	3,914	0,403	5,826	72,931	70,065
66,6094	48,5787	2,23	0,9607	0,701	47,6967	55,03	377,52	0,4824	3,914	0,403	5,826	72,931	70,065
68,0753	49,6478	2,08	0,9607	0,701	44,3808	55,03	377,52	0,4824	3,432	0,401	5,574	72,931	70,065
69,5412	46,1962	1,94	0,9607	0,638	41,3900	55,03	377,52	0,4412	2,991	0,401	5,342	66,430	63,819
64,8930	43,1084	1,98	0,9601	0,638	42,1723	54,61	350,48	0,4412	2,549	0,374	4,841	66,430	63,782
66,1195	43,9232	1,86	0,9601	0,638	39,6962	54,61	350,48	0,4412	2,108	0,378	4,610	66,430	63,782
67,3459	41,3442	2,27	0,9601	0,589	48,4868	54,61	350,48	0,5285	1,580	0,378	4,333	61,391	58,944
82,2888	50,5178	2,32	0,9598	0,589	49,5238	54,37	423,58	0,5285	1,051	0,451	4,787	61,391	58,923
84,0488	51,5982	2,37	0,9598	0,589	50,5609	54,37	423,58	0,5285	0,523	0,451	4,510	61,391	58,923
85,8087	52,6787	0,00	0,9598	0,589	0,0000	54,37	424,58	0,5226	0,000	0,425	4,246	61,391	58,923
2134,95	1655,78	77,56		96,28	1594,20	74,67							

References

1. Xie W.T., Dai Y.I., R.Z. Wang R.Z., Sumathy K. Concentrated solar energy applications using Fresnel lenses: A review. *Renewable and Sustainable Energy Reviews*. 2011. **15**. P. 2588–2606. http://doi.org/10.1016/j.rser.2011.03.031.
2. Rumyantsev V.D. Solar concentrator modules with silicone-on-glass Fresnel lens panels and multijunction cells. *Opt. Exp.* 2010. **18**, No S1. P. A17–A24. http://doi.org/10.1364/OE.18.000A17.
3. Yamada N., Okamoto K. Experimental measurements of a prototype high concentration Fresnel lens CPV module for the harvesting of diffuse solar radiation. *Opt. Exp*. 2014. **22**, No S1. P. 198654. P. A28–A34. https://doi.org/10.1364/OE.22.000A28.
4. Green M.A., Dunlop E.D., Hohl-Ebinger J., Yoshita M., Kopidakis N., Ho-Baillie A.W.Y. Solar cell efficiency tables (Version 55). *Prog. Photovolt. Res. Appl.* 2020. **28**. P. 3–26.
5. Yamaguchi M., Luque A. High efficiency and high concentration in photovoltaics. *IEEE Trans. Electron Devices*. 1999. **46**, No 10. P. 2139–2144. http://doi.org/10.1109/16.792009.
6. Baig H., Heasman K.C., Mallick T.K. Nonuniform illumination in concentrating solar cells. *Renewable and Sustainable Energy Reviews.* 2012. **16**. P. 5890–5909. http://doi.org/10.1016/j.rser.2012.06.020.
7. Ju X., Pan X., Zhang Z. *et al.* Thermal and electrical performance of the dense-array concentrating photovoltaic (DA-CPV) system under nonuniform illumination. *Appl. Energy*. 2019. **250**. P. 904–915. http://doi.org/10.1016/j.apenergy.2019.05.083.
8. Benitez P., Minano J.C., Zamora P. *et al.* High performance Fresnel-based photovoltaic concentrator. *Opt. Exp*. 2010. **18**, No S1. P. A25–A40. http://doi.org/10.1364/OE.18.000A25.
9. Rumyantsev V.D., Ashcheulov Yu.V., Davidyuk N.Yu. *et al.* CPV modules based on lens panels. *Adv. Sci. Technol.* 2010. **74**. P. 211–218. http://doi.org/10.4028/www.scientific.net/AST.74.211.
10. Erismann F. Design of a plastic aspheric Fresnel lens with a spherical shape. *Opt. Eng*. 1997. **36**, No 4. P. 988–991. http://doi.org/10.1117/1.601292.
11. Antonov E.E., Fu M.L., Petrov V.V., Manko D.Yu., Rong K.H. Structure of microprismatic Fresnel lenses for creating uniform focal images. *Opt. Exp.* 2021. **29**, No 24. P. 38958–38970. http://doi.org/10.1364/OE.438590.
12. Petrov V., Kryuchyn A., Antonov E., Lapchuk A., Shanoylo S. Optical phenomena in microprism diagnostic set KK-42. *Proc. SPIE*. 2011. **8011**, No 80119A. *22 General Congress on Optics "ICO-22",* 15–19 August, 2011, Puebla, Mexico. http://doi.org/10.1117/12.900751.
13. Brinksmeier E., Glabe R., Schonemann L. Diamond micro chiseling of large-scale retroreflective arrays. *Precis. Eng*. 2012. **36**. P. 650–657. http://doi.org/10.1016/j.precisioneng.2012.06.001.
14. Le Z.C., Antonov E.E., Mao Q. *et al.* Anti-fatigue glasses based on microprisms for preventing eyestrain. *Sensors*. 2022. **22**, No 5. P. 1933–1948. https://doi.org/10.3390/s22051933.
15. Antonov E.E., Lapchuk A.S., Petrov V.V., Tokalin O.A., Zenin V.N. Photodetector module of optoelectronic control systems for tracking the moving objects. *Semiconductor Physics, Quantum Electronics and Optoelectronics*. 2022. **25**, No 3. P. 315–322. https://doi.org/10.15407/spqeo25.03.315.
16. Born M., Wolf E. *Principles of Optics: Electromagnetic Theory of Propagation, Interference and Diffraction of Light*. 7th ed. Cambridge, Cambridge University Press, 1999. https://doi.org/10.1017/CBO9781139644181.
17. Fu M.L., Antonov E.E., Manko D.Yu., Petrov V.V., Rong K.Z. Microprismatic Fresnel lens for formation of uniform light circle. *IEEE Photonics J*. 2021. **13**, No. 3. P. 2200108. http://doi.org/10.1109/JPHOT.2021.3072538.
18. Sultanova N., Kasarova S., Nikolov I. Dispersion properties of optical polymers. *Acta Physica Polonica A*. 2009. **116**, No 4. P. 585–587. http://doi.org/10.12693/APhysPolA.116.585.
19. Tan N.Y.J., Lim Z.H., Zhou G., Liu K., Kumar A.S. Design and fabrication of composite polygonal Fresnel lenses. *Opt. Exp*. 2021. **29**, No 22. P. 36516–36534. https://doi.org/10.1364/OE.436290.
20. Tan N.Y.J., Neo D.W.K., Zhang X. *et al.* Ultra-precision direct diamond shaping of functional micro features. *J. Manuf. Process*. 2021. **64**. P. 209–223. https://doi.org/10.1016/j.jmapro.2020.12.064.
21. Harmon S. Solar-optical analyses of a mass-produced plastic circular Fresnel lens. *Solar Energy*. 1977. **19**, No 1. P. 105–108. http://doi.org/10.1016/0038-092X(77).90096-2.

Authors and CV

Eugene Antonov graduated from Moscow Physical-Engineering Institute with MS degree in experimental physics. His PhD (1978) is for optics and optical diagnostics. Doctor of Engineering Sciences (2020) for microprism simulation, the leading researcher at the Institute for Information Recording, NAS of Ukraine. Now he specializes in optical properties of microprisms. Dr. Antonov is the author of more than 120 scientific works, including 2 monographs and 13 patents. He awarded by the Cabinet of Ministers of Ukraine (2013), awarded by Special Mark of National Academy of Sciences of Ukraine for professional activity (2017).
E-mail: antv1947@gmail.com,
http://orcid/0000-0003-4471-8287

Sergiy Kondratenko obtained MS Degree in physics in 1998 from Kyiv Taras Shevchenko National University, Ph. degree in 2002 and Doctor of Sciences in 2013 for optics and laser physics. Now he specializes in physics of semiconductors, nanoelectronics and photovoltaics. Authored of more than 130 scientific works, 73 of them are included in Scopus. http://orcid.org/0000-0002-4403-7732. E-mail: kondratenko@knu.ua

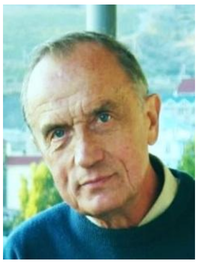

Volodymyr Lysenko obtained MS Degree in physics in 1977 from Kyiv Taras Shevchenko National University, Ph. degree in 1981 and Doctor of Science in 1988 for physics of semiconductors and dielectrics. Corresponding Member of NAS of Ukraine since 1992. Prof. Lysenko is the chief researcher of ISP NAS of Ukraine. His research areas are micro-, nano-, optoelectronics and information technologies; nanoparticles for antiviral and anticancer therapy. V.S. Lysenko is the author of 5 monographs and more than 300 scientific works, 198 of them are included in Scopus. He is a laureate of State Prize of Ukraine, prizes named C.O. Lebedev (2004), V.E. Lashkaryov (2006) and V.M. Glushkov (2021) of National Academy of Sciences of Ukraine. E-mail: lysenko.v@nas.gov.ua, http://orcid.org/0000-0001-9948-9499

Viacheslav Petrov graduated from the Kharkiv Polytechnic Institute in 1962, got DSc degree in 1983, academician of NAS of Ukraine since 2012. Prof. Petrov is the Director of the Institute for Information Recording, NAS of Ukraine. Research interests of V. Petrov are the long-term storage of digital information, microprisms for ophthalmology applications, scientometrics, applied optics. He is the author of more than 600 scientific works, including 8 monographs and more than 230 patents, awarded by 16 Ukrainian and international awards.
E-mail: petrov@ipri.kiev.ua,
http://orcid.org/0000-0002-7265-9889

Vladimir Zenin graduated from the Kyiv Polytechnic Institute. He is working at the Institute for Information Recording from 1992 till now. V. Zenin is the researcher at IIR NAS of Ukraine. Carried out a series of design and research works on the development of technological equipment for implementation of diamond microcutting method, investigated the optical properties of retroreflective devices and homogenizer for optical radiation. V. Zenin is the author of more than 40 scientific works and patents.
E-mail: zen51vlad@gmail.com

Authors' contributions

Antonov E.E.: conceptualization, formal analysis, investigation, validation, writing – original draft, visualization.
Kondratenko S.V.: formal analysis, investigation, validation, writing – review & editing, visualization.
Lysenko V.S.: conceptualization, methodology, formal analysis, supervision, writing – review & editing.
Petrov V.V.: investigation, project administration, supervision, writing – review & editing.
Zenin V.N.: investigation, validation, software and hardware.

Мікропризматичні плоско-фокусуючі лінзи Френеля для концентрації світла в сонячних фотоелектричних модулях

Є.Є. Антонов, С.В. Кондратенко, В.С. Лисенко, В.В. Петров, В.М. Зенін

Анотація. Розроблено алгоритм моделювання параметрів мікропризматичних спеціалізованих плоско-фокусуючих лінз Френеля. Такі лінзи більш ефективні для застосування у фотоелектричних модулях для концентрації сонячного світла порівняно з традиційними точковими лінзами Френеля. Досліджено технічні параметри фотоелектричних модулів з такими лінзами. Запропоновано спосіб виготовлення вищезазначених лінз методом алмазного мікроточіння з подальшим термічним пресуванням силіконових заготовок. Експериментально досліджено окремі зразки спеціалізованих мікропризм плоского фокусування, виготовлених за результатами нашого моделювання.

Ключові слова: мікропризматична структура, моделювання плоско-фокусуючої оптики, фотоелектричне перетворення сонячного світла.